Evaluation of Tension in Actin Bundle of Endothelial Cells Based on Preexisting Strain and Tensile Properties Measurements

S. Deguchi [1,2], **T. Ohashi** [2], **and M. Sato**[2]

Abstract: Actin bundles in vascular endothelial cells (ECs) play a critical role in transmitting intracellular forces between separate focal adhesion sites. However, quantitative descriptions of tension level in single actin bundles in a physiological condition are still poorly studied. Here, we evaluated magnitude of preexisting tension in a single actin bundle of ECs on the basis of measurements of its preexisting stretching strain and tensile properties. Cultured ECs expressing fluorescently-labeled actin were treated with detergents to extract acin bundles. One end of an actin bundle was then dislodged from the substrate by using a microneedle, resulting in a shortening of the actin bundle due to a release of preexisting tension. Assuming the shortened actin bundle reached its non-stress state, preexisting stretching strain was determined to be 0.24 on average. A tensile test of the dislodged single acin bundle was conducted with a pair of cantilevers to measure the force required for stretching it up to the original length, yielding an estimate of preexisting tension in the actin bundle. The magnitude of the preexisting tension, 4 nN on average, was comparable to previously reported data of the traction force generated by adherent cells at single adhesion sites to keep cell integrity. The Young's modulus of the isolated actin bundle was estimated to be ∼300 kPa from the tensile tests together with evaluation of average diameter of the isolated actin bundle based on transmission electron microscopy. These data will contribute to better understanding of intracellular stress transmission mechanism in ECs.

keyword: Actin bundle, Dense peripheral band, Stress fiber, endothelial cell, Intracellular stress, Yong's modulus, Mechanotransduction.

---

[1] Corresponding author. Department of Energy Systems Engineering, Graduate School of Natural Science and Technology, Okayama University, Okayama, Japan. Address: Tsushima-naka 3-1-1, Okayama 7008530, Japan; Phone: +81 86 251 8053; Fax: +81 86 251 8266; E-mail: deguchi@mech.okayama-u.ac.jp

[2] Department of Bioengineering and Robotics, Tohoku University, Sendai, Japan

1 Introduction

Adaptation of vascular endothelial cells (ECs) to mechanical stimuli has been reported in many studies (Levesque and Nerem, 1985; Davies, 1995; Sato et al., 2000; Li et al, 2002; Davies et al, 2003; Deguchi et al, 2005). For instance, when exposed to fluid shear stress, biochemical responses appear in the cells, which align the cells and their actin filaments in the direction of flow. The accurate mechanism of such cellular directional responses remains elusive. However, it has been proposed and gained increasing attention that intracellular forces due to mechanical stimuli are transmitted over the cytoplasm as a mechanical pathway along with biochemical pathways to help in giving a mechanical signal such as tension to localized mechano-sensing sites such as focal adhesions (Davies, 1995, 2003; Ingber, 1997, 2004).

To elucidate the mechanical pathway, it is of importance to understand the cell mechanical structure, in other words, how structure of the adherent cell is constructed from what subcellular structural components. Here, we focus on actin bundles as such structural components in ECs. Actin bundles are composed of actin filaments grouped together with myosin, vinculin, and other actin-binding proteins to form a thick fiber with a diameter of several hundred microns (Burridge, 1981; Byers and Fujiwara, 1982; Wong and Gotlieb, 1986; Satcher and Dewey, 1996; Furukawa and Fechheimer, 1997; Katoh et al., 1998, 2000; Deguchi et al., 2005). Some actin bundles are often localized around the cell periphery in cultured and confluent ECs, which is referred to as dense peripheral band (Levesque and Nerem, 1985; Wong and Gotlieb, 1986). In contrast, the other thick actin bundles, which often develop in mechanical stress-imposed condition and run transversely across the cytoplasm, is referred to as stress fiber (Levesque and Nerem, 1985; Burridge, 1981; Byers and Fujiwara, 1982). Immunostaining patterns of actin-binding proteins were similar between dense peripheral band and stress fiber (Wong and Gotlieb, 1986). In addition, their dynamic behaviors

were sometimes hardly distinguishable (Li et al., 2002). In the present study, therefore, we will not distinguish them but will refer to as actin bundle.

Importantly for considering the cell mechanical structure, cells drag the substrate surface toward the cell center to keep their structural integrity (Ingber, 1997, 2004; Pourati et al., 1998; Tan et al., 2003; Lemmon et al., 2005). The motive power of the pull (or traction force) is actomyosin contraction-based isomeric tension in the actin bundles (Burridge, 1981; Katoh et al., 1998, 2000; Tan et al., 2003). Both ends of actin bundle are anchored to the stiff substrate (i.e., glass or plastic surface in vitro and the basement membrane in vivo) via the focal adhesions. The distance between the two focal adhesions, each located at each end of actin bundle, does not change in statically cultured condition, thus producing isometric tension. Although the isometric tension would be a critical factor in considering the cell structure, mechanical properties of actin bundle of ECs and magnitude of its tension remain mainly unclear.

We have previously reported that stress fibers in smooth muscle cells shortened after they had been extracted from the cells and isolated form the substrate (Deguchi et al., 2005). The shortening was caused by a release of pre-existing tension in stress fibers that presumably comes from the isometric tension due to actomyosin contraction. The magnitude of force required for stretching the isolated single stress fiber from the tension-released (i.e., non-stress) state to its original length was ∼10 nN. The force magnitude was comparable with that of the traction force of adherent smooth muscle cells (Tan et al., 2003), suggesting that the preexisting tension in stress fibers is closely associated with the traction force. However, quantitative description of magnitude of the tension in actin bundles of ECs has not yet appeared although better understanding of intracellular force balance in ECs is an important issue.

In the present study, we evaluated preexisting tension in actin bundle of ECs. We first investigated preexisting strain of actin bundle after chemically and mechanically isolated from the cells and the substrate. Tensile tests of the isolated actin bundles were then conducted to measure the force required for keeping the preexisting strain. The Young's modulus of the actin bundle was determined taking into account its average diameter obtained from electron microscopy to establish macroscopic and averaged mechanical properties. These data will contribute to elucidating the cell structure as well as intracellular stress transmission mechanism.

2 Materials and Methods

2.1 Cell preparation

Freshly excised bovine thoracic aortas were obtained from a local slaughterhouse. ECs were isolated according to the reported technique (Shasby and Shasby, 1987). Cells were cultured in Dulbecco's modified Eagle medium (DMEM, Invitrogen) supplemented with 10% fetal bovine serum (FBS, JRH Biosciences) and 1% each of penicillin and streptomycin. Cells were used at passages 5–12. Cells were co-transfected with pEGFP-actin vector (GFP-actin, Clontech) and pdsFP593-focal adhesion targeting vector (RFP-FAT, a gift of Dr. N. Mochizuki, National Cardiovascular Center, Japan; FAT, an amid acid sequence at C-terminus of focal adhesion kinase) using a liposomal method. At 24 h after passage, cells were incubated with a mixture of the DNA plasmids, Lipofectamin (Invitrogen), and Plus Reagent (Invitrogen) in a serum-free medium (Opti-MEM, Invitrogen) for 5 h. After the mixture was replaced with FBS-containing DMEM, cells were incubated in a humidified 5% CO_2 atmosphere at 37^oC overnight. Before experiments, cells expressing GFP-actin and RFP-FAT were incubated with a buffer A (10 mM imidazole (Wako), 100 mM KCl, and 2 mM EGTA (Wako), pH 7.2) containing 25 μg/ml saponin (Wako) for 8 min at 37^oC to remove intracellular ATP and cations, which induce actomyosin-based contraction (Katoh et al., 1998, 2000).

2.2 Extraction of actin bundle

Culture medium was washed with a PBS containing 1 μg/ml each of leupeptin and pepstatin and kept at 4^oC. To extract actin bundles according to the reported technique (Katoh et al., 1998, 2000), cells were treated with a low-ionic-strength extraction solution (2.5 mM triethanolamine and 1 μg/ml each of leupeptin and pepstatin in distilled water) for 20–40 min, the PBS with 0.05% NP-40 (pH 7.2) for 5 min, and the PBS with 0.05% Triton X-100 (pH 7.2) for 5 min. Extracted actin bundles were then washed gently with the PBS to remove the detergents.
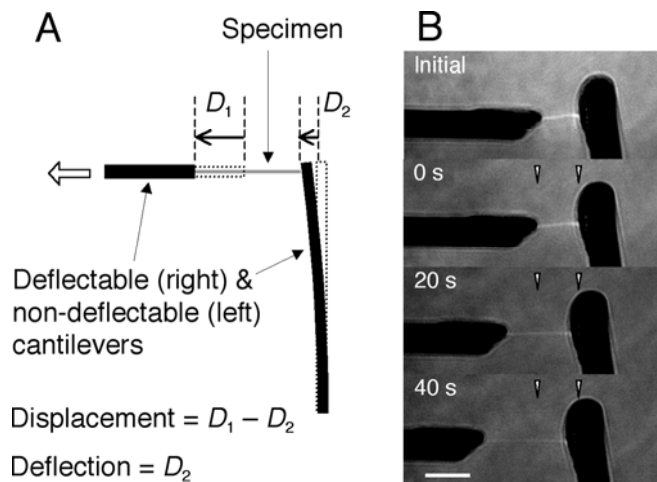
Figure 1 : Tensile test of a single actin bundle isolated from ECs. (A) Schematic diagram. (B) Sequential images. An actin bundle captured by a pair of cantilevers was in a slack state before being stretched (Initial) and was gradually stretched owing to movements of the left cantilever (0, 20, and 40 s). Arrowheads show original positions of the cantilevers. Scale bar = 20 μm.

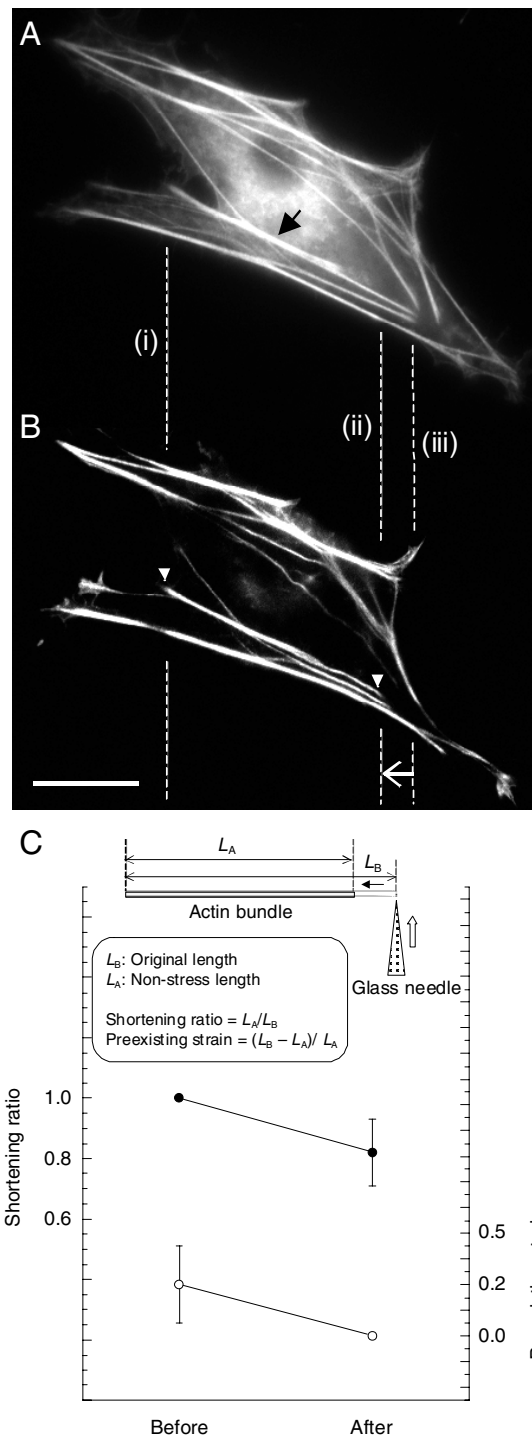### 2.3 Evaluation of preexisting strain of actin bundle

The dish with the cells was placed on a stage of an inverted microscope (IX-70, Olympus). The actin bundle extraction treatments were performed while the dish was being fixed on the stage. After the extraction, the PBS were replaced with the buffer A. Oxygen-removal reagents (2.3 mg/ml glucose, 0.018mg/ml catalase, and 0.1mg/ml glucose oxidase) (Kishino and Yanagida, 1988) were added to reduce photo-bleach. By manipulating a fine glass needle made of a capillary tube, one of the focal adhesions visualized by RFP-FAT was carefully dislodged from the substrate surface as previously applied to dislodging cell processes similarly (Pourati et al., 1998). For more detail, the needle was placed underneath the vicinity of a targeted focal adhesion site and slid slightly across the target to scrape it off from the ground. Fluorescence images were acquired by a CCD camera (C4742-95ER, Hamamatsu Photonics) to examine changes in length of actin bundle. The lengths were determined by manually tracing actin bundle images from one end to the other end with the NIH image software (Version 1.62).

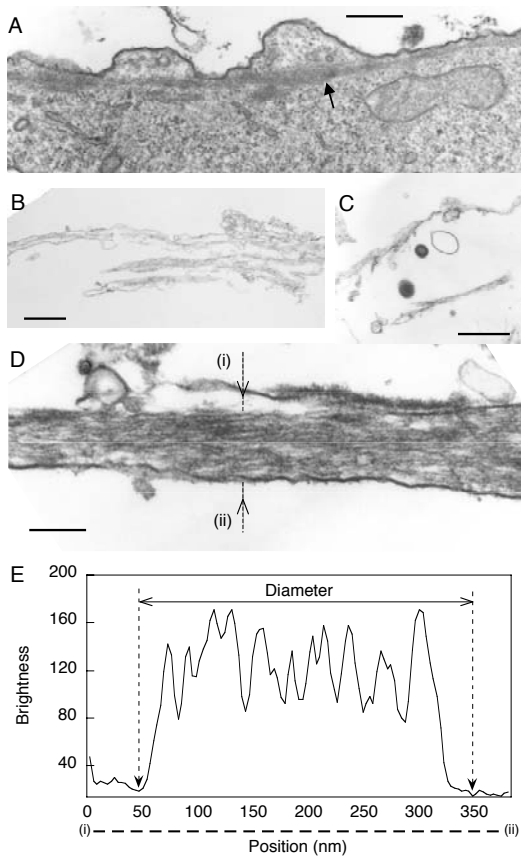### 2.4 Evaluation of diameter of actin bundle

Transmission electron microscopy was conducted to evaluate average diameter of isolated actin bundles. The chemically extracted actin bundles were fixed with fresh 2.5% glutaraldehyde, 2% paraformaldehyde, and 0.5% tannic acid in 0.1 M cacodylate buffer (pH 7.4) for 24 h at 4°C, rinsed with 0.1 M cacodylate buffer for 1 h at 4°C, scraped off from the dish by using a rubber scraper, post-fixed with 1% osmium tetroxide in the same buffer for 1 h at 4°C, dehydrated through a graded series of ethanol (60, 70, 80, 90, and 100%), infiltrated with n-butyl glycidyl ether, embedded in Epon812, and cut with an ultra-microtome. Ultra-thin sections were mounted onto copper grids, stained with aqueous uranyl acetate and lead citrate, and observed by a transmission electron microscope (H-7100, Hitachi) at an accelerating voltage of 75 kV. Diameter of the isolated actin bundles was estimated from electron microscopic images with a 256 gray scale by using the NIH image software. A line was drawn perpendicular to an actin bundle on the image to measure brightness on the line. Edge of the actin bundle was detected from a substantial change in the brightness distribution between the actin bundle and the background, and thus the diameter was determined as the distance between the detected edges. The diameter was examined at 80 points out of 8 isolated actin bundles

2.5 Tensile test of actin bundle

Extracted actin bundles were scraped off from the dish by using a rubber scraper (Sumilon). Tensile tests of the isolated actin bundles were carried out in the buffer A supplemented with the oxygen-removal reagents at room temperature (20°C) on an inverted microscope (IX-71, Olympus) with the previously reported technique (Deguchi et al., 2005). Briefly, a deflectable cantilever made of a flexible carbon fiber (7 μm in diameter and $\sim$0.5–1.5 mm in length) attached to a tip of a rigid glass rod (1 mm in diameter) was used to hold one end of a single actin bundle (Fig. 1A). Another cantilever was used to fix the position of the other end. Prior to experiments, an epoxy adhesive was thinly coated on the tips of the cantilevers. Both ends of the specimen were then captured by the cantilevers under illuminations from halogen and mercury light sources. The non-deflectable cantilever was moved by using a piezo-electric actuator connected to the base of the cantilever to stretch the specimen at a constant strain rate of 0.02 s^{-1} while ac-
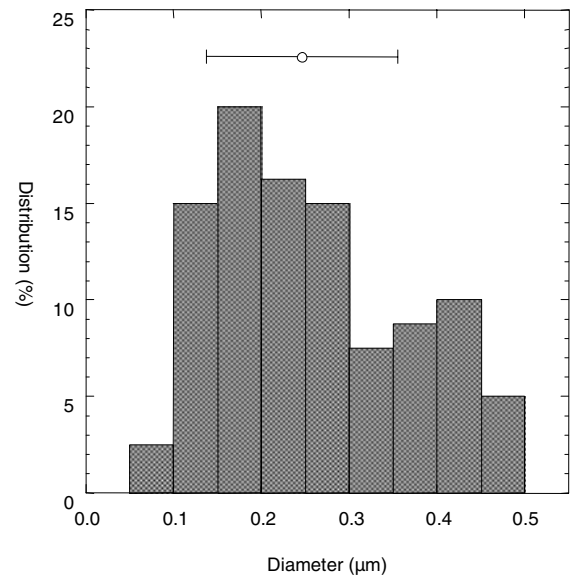
Figure 2 : Preexisting strain of actin bundles. (A, B) GFP-actin images of a cultured EC before (A) and after (B) the treatments of the chemical extraction and the glass needle manipulation. After the right end of an actin bundle (arrow in A; each end, arrowheads in B) had been dislodged from the substrate, it was displaced from a point on the line (iii) to another on the line (ii) presumably due to a release of preexisting tension in the actin bundle. On the other hand, the left end, which was not dislodged, remained stayed on the line (i). Scale bar =10 μm. (C) Shortening ratio (●, the left ordinate) and preexisting strain (○, the right ordinate) before and after the treatments. Mean $\pm$ SD (n = 11).

Figure 3 : Evaluation of diameter of actin bundles based on transmission electron microscopy. (A–D) Electron micrographs of actin bundles. Ultra-structural features of actin bundles in the cell (arrow in A) were preserved in the isolated states (B–D). Scale bars in A–C = 1 μm. Scale bar in D = 200 nm. (E) Determination of diameter of actin bundle. Brightness was measured on a line drawn perpendicular to an actin bundle ((i)–(ii) in D). The edges of the actin bundle were defined by the positions where a substantial change in brightness was obtained (vertical dashed arrows in E), and the diameter was determined by the distance between the points. The brightness was expressed by 256 gradients.

quiring the images by a CCD camera. Deflection of the deflectable cantilever and displacement of the specimen were obtained from the images by using the NIH image software. Tensile load was determined from the deflection of the deflectable cantilever multiplied by cantilever stiffness (1–7 nN/μm) obtained from cross-calibration (Kishino and Yanagida, 1988).


Figure 4 : Histogram of the diameter of actin bundles. A plot and a horizontal bar indicate mean and standard deviation (n = 80) of the diameter, respectively.

3 Results

3.1 *Preexisting strain*

The cells were almost confluent at experiments, and many of the thick actin bundles were localized around the cell periphery. The cell membrane and cytoplasmic constituents including the nucleus were removed after the chemical treatments, and actin bundles were extracted. To confirm whether actin bundles carry preexisting tension, we observed shape changes after the extracted actin bundle had been detached at one end from the substrate. After detached owing to the glass needle manipulation, the actin bundles shrank somewhat like a recoil of an elastic material (Fig. 2A and B). The shrink is attributable to a sudden release of preexisting tension in the actin bundle as observed similarly in the cell process in previous studies (Pourati et al., 1998). Assuming that the detached actin bundle finally reached its non-stress state, we examined magnitude of the shortening. The ratio of initial length (before detachment) to non-stress length (after detachment) was 0.82 ± 0.11 (mean $\pm$ SD, n = 11) (Fig. 2C). If we define preexisting strain as ((initial length) - (non-stress length))/(non-stress length), actin bundles had a preexisting stretching strain of 0.24 ± 0.18 before extraction (Fig. 2C).

A   **B**
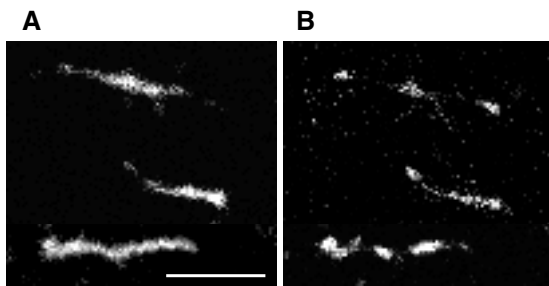
Figure 5 : Double staining of isolated actin bundles with rhodamine-phalloidin (A) and a monoclonal antibody against vinculin (B). Scale bar = 10 μm.

3.2 Diameter

The electron microscopy showed that ultra-structural features of actin bundles in the cell (i.e., thick fibers composed of bundled actin filaments (Fig. 3A)) were preserved after isolation (Fig. 3B–D). Electron micrographs of the isolated actin bundle were used to examine an average value of its diameter. Comparison of brightness line profiles measured along a line drawn perpendicular to an actin bundle showed a definite difference between the actin bundle- and the background-regions (Fig. 3D and E). The transition points were used to determine both edges of the actin bundle. Diameter of the isolated actin bundles was thus estimated to be 0.25 $\pm$ 0.11 μm (mean $\pm$ SD, n = 80) (Fig. 4). Assuming that the cross-section is idealized as a circle with the average diameter, we determined a representative cross-sectional area of the isolated actin bundle to be 0.049 μm^2.

3.3 Tensile properties and preexisting tension

The chemically extracted actin bundles were scraped off from the substrate before tensile test. We confirmed in separate experiments with a monoclonal antibody against vinculin that the isolated actin bundles were still associated with vincluin as in vivo (Fig. 5). The isolated single actin bundles were stretched in the tensile tests from the non-stress state up to a strain (defined as the ratio of displacement to initial length) of > 1.0 across the preexisting strain level (i.e., 0.24 on average (Fig. 2C)). The deflectable cantilever was gradually bent since tensile load was given via the actin bundle (Fig. 1B). Force–strain relations were then obtained and averaged in a 0.0–1.0-strain range at a 0.1-strain interval (n = 6, Fig. 5). Initial length of the specimen was 10.3 $\pm$ 2.8 μm. In a higher

stretching strain range of > 0.1, tensed actin bundles detached at one end from either of the cantilevers.

The mean force plots (Fig. 6, circles) were fitted to a quadratic expression by the least-squares method to obtain a regression curve of the force (F)–strain (S) relationship, $F = 12.7S^2 + 14.2\,S$ (nN). The correlation coefficient R^2 was equal to 0.997 in the analysis. By substituting $S = 0.00$ or $S = 0.237$ (≈ 0.24 (Fig. 2C)) into the first derivative dF/dS, we obtained stretching stiffness as 14.2 (nN) at the non-stress state or 20.2 (nN) at the pre-tensed state, respectively. If D (μm) is a diameter of an isolated actin bundle cross-section assumed to be a homogeneous circle, the incremental elastic modulus (E) is calculated as $E = 4 \times \mathrm{d}F/\mathrm{d}S /(\pi D^2)$ (kPa) (Fig. 7). Hence, if $D = 0.251$ (≈ 0.25 (Fig. 4)) μm, the elastic modulus is 287 kPa at the non-stress state (that represents the Young's modulus of the isolated actin bundle) or 408 kPa at the pre-tensed state. By substituting the average preexisting strain 0.237 for S of the regression curve, preexisting tension level was estimated to be 4.08 nN (Fig. 6).

4 Discussion

Actin bundles of ECs produce actomyosin contraction-based isometric tension (Burridge, 1981; Katoh et al., 1998), which would play a critical role in maintenance of cell structural integrity as well as transmission of intracellular stress (Ingber, 1997, 2004). However, the tension has not been well-studied from quantitative viewpoints. The principal purpose of the present study is therefore to evaluate magnitude of the tension in single actin bundles for better understanding of the cell structure. The strategy was first to identify preexisting stretching strain of single actin bundle by making it free from surrounding mechanical constraints (i.e., the cell membrane, the other cytoplasmic constituents, and the substrate) to observe resultant shortening, then to measure its tensile force–strain relation, and lastly to examine the average tensile force required for keeping preexisting strain to evaluate preexisting tension. In addition, to further evaluate magnitude of elastic modulus of the actin bundle, its average diameter was measured from electron microscopy.
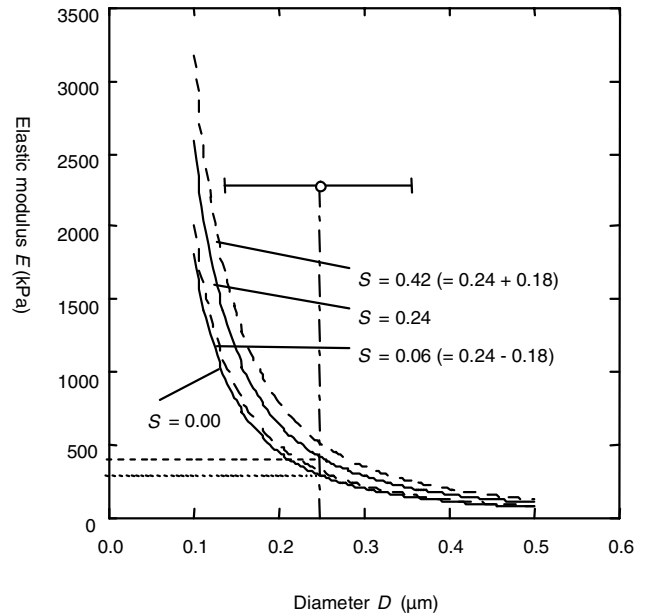
The result showed that preexisting tension was estimated $\sim$4 nN on average (Fig. 6). Tan et al. (2003) measured traction force of adherent ECs applied to the substrate at single focal adhesion sites to obtain an $\sim$10-nN traction force, the order of which is comparable to that of the estimated preexisting tension in single actin bundles. In con-
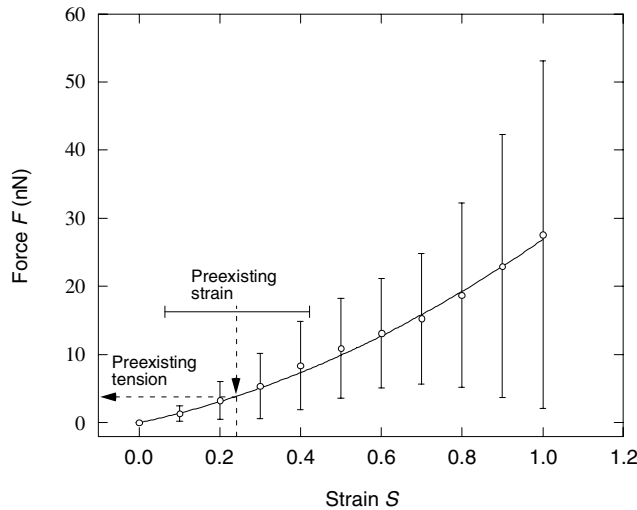
Figure 6 : Relationship between tensile force and stretching strain. Vertical solid bars indicate standard deviation (n = 6). Means were obtained at every 0.1 strain. A curve was obtained by the least-squares regression for the mean plots. A horizontal solid bar and a vertical dashed line indicate standard deviation and mean of pre-existing strain, respectively. A horizontal dashed arrow indicates an estimated preexisting tension.

Figure 7 : Relationship between elastic modulus and diameter. A parameter S indicates the stretching strain of actin bundle. A vertical dashed line and a horizontal solid bar indicate mean and standard deviation of diameter obtained in the electron microscopy, respectively. Two kinds of horizontal dashed lines indicate levels of incremental elastic modulus corresponding to their strain levels.

trast, actin microfilament, which is a major component of actin bundles, can bear a tensile force of at most 600 pN (Tsuda et al., 1996) that would be insufficient for bearing the traction force. Hence, the quantitative comparison suggests that the principal component responsible for the traction force or the mechanical integrity at the cell bottom is most likely to be 'bundled' actin filaments.

Since diameter of the actin bundles is of submicron order of magnitude, it was difficult to directly measure the diameter of individual actin bundles from the phase-contrast or fluorescence microscopy during the tensile tests. The diameter was therefore evaluated from a separate experiment with electron microscopy to investigate the order of its average value although diameters of individual specimens cannot be specified. The electron microscopy showed that the diameter was quite variable (Fig. 3). Such variations in the morphology and composites of the specimen might be a major factor responsible for data dispersions in the mechanical tests (Figs. 2 and 6). Specification of the relation between mechanical properties and the morphology or composite of each specimen will be the subject of future investigation.

The Young's modulus of the actin bundle was determined to be 287 kPa assuming a uniform circle cross-section with the average diameter (0.25 μm) (Fig. 7). If we take the dispersion of the diameter (Fig. 4) into account, the Young's modulus would lie in a range from > 100 kPa to ~ 1 MPa (Fig. 7). Incremental elastic modulus was also evaluated at the preexisting strain level (i.e., $S = 0.24$) to be 408 kPa. Dispersion of the preexisting strain (Fig. 2) causes variations of the elastic modulus at the average diameter, e.g., $S = 0.42$ (= 0.24 + 0.18 (i.e., mean + SD)) yields 508 kPa, and $S = 0.06$ (= 0.24 − 0.18) yields 320 kPa (Fig. 7). Thus, we examined a possible range of the elastic modulus to establish macroscopic and averaged mechanical properties. To our knowledge, this is the first quantitative description of mechanical properties of single actin bundles isolated from ECs. The Young's modulus of the actin bundle was almost three orders of magnitude smaller than that of its principal component, actin filament, which has an ~ 1 GPa Young's modulus

according to previous reports (Gittes et al., 1993; Kojima et al., 1994); however, the mechanism of the difference remains unclear.

We previously reported preexisting strain and tensile properties of single stress fibers isolated from cultured smooth muscle cells (Deguchi et al., 2005). The results showed that preexisting strain magnitude was almost consistent between actin bundles of ECs (i.e., 0.24) and stress fibers of smooth muscle cells (i.e., 0.21), implicating that basic mechanism for establishing the cell architecture might be similar between ECs and smooth muscle cells although physiological functions are different to each other. By contrast, stretching stiffness of the former (i.e., 14.2 nN) was almost 30% of that of the latter (i.e., 45.7 nN). Although the diameter of the stress fiber was not evaluated in the previous study, the difference of the stiffness might be partly attributable to the cross-section size of the specimens in addition to difference in the composites because larger size corresponds to greater stiffness.

5 Summary

We measured preexisting strain and tensile properties of actin bundle of ECs to understand its macroscopic and average mechanical behavior. Actin bundles shortened after they had been detached from the substrate in an ATP-independent manner to ~80% of the original length, indicating that a stretching strain of 0.24 on average may exist in the actin bundles in the cytoplasm. Tensile test showed that the isolated actin bundle had a 287-kPa Young's modulus assuming that its diameter was 0.25 μm based on electron microscopy. Tensile force level existing in actin bundle in the cells was then estimated to be 4 nN on the basis of the force–strain relationship. These findings will be important for better understating of contributions of actin bundles to intracellular stress transmission from quantitative viewpoints.

References

Burridge, K. (1981): Are stress fibers contractile? *Nature*, vol. 294, pp. 691–692.

Byers, H.R. and Fujiwara, K. (1982): Stress fibers in cells in situ: immunofluorescence visualization with anti-actin, antimyosin, and anti-alpha-actinin. *Journal of Cell Biol*ogy, vol. 93, pp. 804–811.

Davies, P. F. (1995): Flow-mediated endothelial mechanotransduction. *Physiological Rev*iew, vol. 75, pp. 519–560.

Davies, P. F., Zilberberg, J., and Helmke, B. P. (2003): Spatial microstimuli in endothelial mechanosignaling. *Circulation Research*, vol. 92, pp. 359–370.

Deguchi, S., Maeda, K., Ohashi T., and Sato, M. (2005): Flow-induced hardening of endothelial nucleus as an intracellular stress-bearing organelle, *Journal of Biomechanics*, vol. 38, pp. 1751–1759.

Deguchi, S., Ohashi, T., and Sato, M., (2005): Tensile Properties of Single Stress Fibers Isolated from Cultured Vascular Smooth Muscle Cells, *Journal of Biomechanics*, in press.

Furukawa, R. and Fechheimer, M. (1997): The structure, function, and assembly of actin filament bundles. *International Review of Cytol*ogy, vol. 175, pp. 29–90.

Gittes, F., Mickey B., Nettleton, J., and Howard, J. (1993): Flexural rigidity of microtubules and actin filaments measured from thermal fluctuations in shape. *Journal of Cell Biol*ogy, vol. 120, pp. 923–934.

Ingber, D. E. (1997): Tensegrity: the architectural basis of cellular mechanotransduction. *Annual Review of Physiology*, vol. 59, pp. 575–599.

Ingber, D. E. (2004): The mechanochemical basis of cell and tissue regulation, Mechanics & Chemistry of Biosystems, vol. 1, pp. 53–68.

Katoh, K., Kano, Y., Masuda, M., Onishi, H., and Fujiwara, K. (1998): Isolation and contraction of the stress fiber. *Molecular Biology of the Cell*, vol. 9, pp. 1919–1938.

Katoh, K., Kano, Y., and Fujiwara, K. (2000): Isolation and in vitro contraction of stress fibers. *Methods in enzymol*ogy, vol. 325, pp. 369–380.

Kishino, A. and Yanagida, T. (1988): Force measurements by micromanipulation of a single actin filament by glass needles. *Nature*, vol. 334, pp. 74–76.

Kojima, H., Ishijima, A., and Yanagida, T. (1994): Direct measurement of stiffness of single actin filaments with and without tropomyosin by in vitro nanomanipulation. *Proceedings of the Natural Academy of Sciences USA*, vol. 91, pp. 12962–12966.

Lemmon, C. A., Sniadecki, N. J. Ruiz, S. A., Tan, J. L., Romer, L. H., and Chen, C. S. (2005): Shear force at the cell-matrix interface: Enhanced analysis for microfabricated post array detectors, *Mechanics & Chemistry of Biosystems*, vol. 2, pp. 1–16.

Levesque, M. J. and Nerem, R. M. (1985): The elongation and orientation of cultured endothelial cell in response to shear stress. *Journal of Biomechanical Eng*ineering, vol. 107, pp. 341–347.

Li, S., Butler, P., Wang, Y., Hu, Y., Han D. C., Usami, S., Guan, J. L., and Chien, S. (2002): The role of the dynamics of focal adhesion kinase in the mechanotaxis of endothelial cells. *Proceedings of the Natural Academy of Sciences USA*, vol. 99, pp. 3546-3551.

Pourati, J., Maniotis, A., Spiegel, D., Schaffer, J. L., Butler, J. P., Fredberg, J. J., Ingber, D. E., Stamenovic, D., and Wang, N. (1998): Is cytoskeletal tension a major determinant of cell deformability in adherent endothelial cells? *American Journal of Physiology–Cell Physio*logy, vol. 274, pp. C1283–C1289.

Satcher, R. L. Jr. and Dewey, C. F. Jr. (1996): Theoretical estimates of mechanical properties of the endothelial cell cytoskeleton. *Biophysical Journal*, vol. 71, pp. 109–118.

Sato, M., Nagayama, K., Kataoka, N., Sasaki, M., and Hane, K. (2000): Local mechanical properties measured by atomic force microscopy for cultured bovine endothelial cells exposed to shear stress. *Journal of Biomechanics*, vol. 33, pp. 127–135.

Shasby, D. M. and Shasby, M. W. (1987): Effect of albumin concentration on endothelial albumin transportation in vitro, *American Journal of Physiology*, vol. 253, pp. H654–H661.

Tan, J. L., Tien, J., Pirone, D. M., Gray, D. S., Bhadriraju, K., and Chen, C. S. (2003): Cells lying on a bed of microneedles: an approach to isolate mechanical force. *Proceedings of the Natural Academy of Sciences USA*, vol. 100, pp. 1484–1489.

Tsuda, Y., Yasutake, H., Ishijima, A., and Yanagida, T. (1996): Torsional rigidity of single actin filaments and actin-actin bond breaking force under torsion measured directly by in vitro micromanipulation. *Proceedings of the Natural Academy of Sciences USA*, vol. 93, pp. 12937–12942.

Wong, M. K. and Gotlieb, A. I. (1986): Endothelial cell monolayer integrity. I. Characterization of dense peripheral band of microfilaments. *Arteriosclerosis*, vol. 6, pp. 212–219.